JOURNAL OF MATERIALS SCIENCE 13 (1978) 1490–1498

Creep, repeated loading, fatigue and crack growth in ± 45° oriented carbon fibre reinforced plastics

J. B. STURGEON
Materials Department, Royal Aircraft Establishment, Farnborough, Hampshire, UK

Tensile creep, intermittent and cyclic fatigue loadings have been applied at room temperature to ±45° orientations of carbon fibre reinforced plastic. Tensile creep tests have also been performed at 50° C. For this angle-plied orientation, where the matrix and the fibre–resin interface are loaded in shear, considerable creep was observed under all three types of loading. During cyclic fatigue tests cracking was observed towards the end of the specimen lifetime. An empirical relation between displacement of the fatigue machine actuator and the remaining lifetime has been derived. From this relation an estimate of cracking growth rate can be obtained.

1. Introduction

Preliminary creep and fatigue tests on 0° unidirectional carbon fibre reinforced plastic (CFRP) have been reported [1, 2]. These, together with tests on 0 + 90° orientations [3, 4], give some indication of the material's potential but no indication of the behaviour of more complex multi-angled constructions such as 0 ± 45°, 0 ± 45° + 90° and 90° ± 45° laminates which are used in engineering applications. Some torsional and flexural tests have been reported for ±45° material [5] but tensile data is lacking, particularly with relation to creep and fatigue interactions, consequently tensile creep, intermittent creep loading and fatigue tests have been made on ±45° orientations of CFRP as part of a programme investigating multi-angled laminates.

2. Materials

The composite materials were supplied by Fothergill and Harvey Ltd in the form of preimpregnated "Carboform" sheets which contained high strength (type 2) surface treated carbon fibres in an epoxy-resin matrix DX210/$BF_3$400, a precondensate system based on a Shell Chemicals Ltd bisphenol-A epoxy.

Laminates were constructed from alternate plies of prepreg to make a balanced lay-up of +45°, −45°, +45°, −45°, −45°, +45°, −45°, +45°. These were consolidated and cured in an autoclave, details are given in [6].

Six specimens were used to find the average monotonic strength which was 161 MPa with a coefficient of variation of 4%.

3. Creep tests

3.1. The creep specimen and testing technique

Rectangular sectioned specimens of dimensions 230 × 25 × 2 mm were used for creep and repeated loading tests. They were accurately aligned in a jig and bonded to aluminium end-pieces which had been drilled to accept shear loading pin attachments for 50 kN Denison creep machines. A free length, 140 mm long, remained unsupported between the end-pieces and strains were measured with Lamb-type optical extensometers having a sensitivity of 2 microstrain over a central 50 mm gauge length. Small aluminium tabs were bonded to each specimen to prevent surface damage by the extensometer fixing points.

3.2. The response of ± 45° CFRP and intermittent loading

Figs. 1–3 show creep and recovery for stress levels of 50, 75 and 100 MPa at 21° C. The elastic strain on first loading has been included and unloadings were made to a small positive stress to maintain

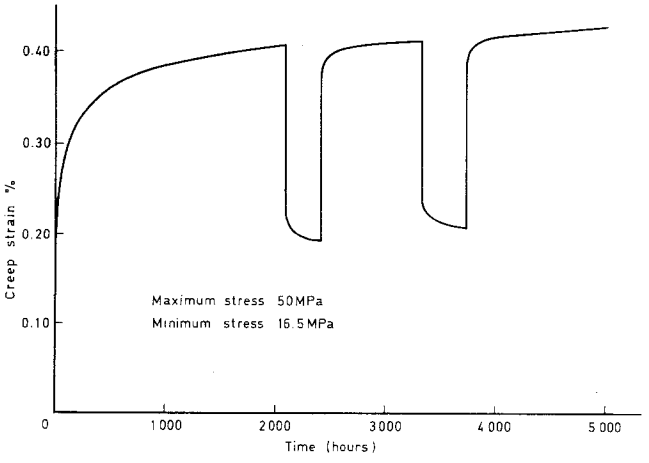

Figure 1 Creep strains for interrupted loading of ± 45° CFRP at 21° C.

TABLE I Instantaneous strains on loading and unloading at 21° C

Maximum stress (MPa)	Loading cycle	Instantaneous strain on loading (%)	Time under load (h)	Unloading cycle	Instantaneous strain recovered on unloading (%)	Recovery time (h)
50	1	0.190	2087	1	0.260	312
	2	0.260	936	2	0.245	408
	3	0.255	1370			
75	1	0.362	2066	1	0.390	406
	2	0.397	840	2	0.384	386
	3	0.388	1370			
100	1	0.701	2253	1	0.520	2030

stability. A summary of the instantaneous deformations is given in Table I, where the instantaneous recovery and reloading strains are factored as though unloading to zero stress had been achieved, the figures on the other hand show the actual strains recorded.

Three points emerge from this data.

Firstly, the creep follows a typical "classical" curve with an initial rapid primary creep which decreases with time followed by a secondary almost constant creep rate.

Secondly, the data of Table I show that proportionately less instantaneous strain is recovered on the first unloading from high stress levels compared with lower stresses.

Thirdly, large permanent creep deformations

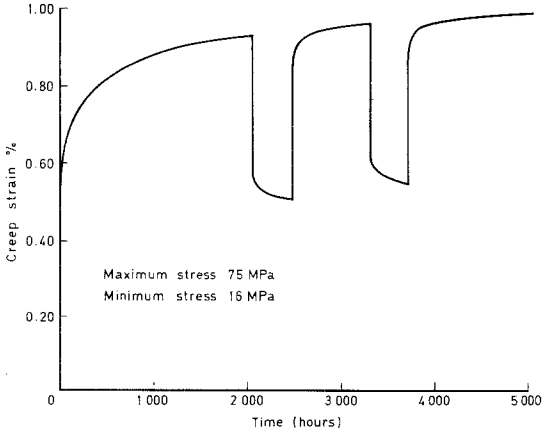

Figure 2 Creep strains for interrupted loading of ± 45° CFRP at 21° C.

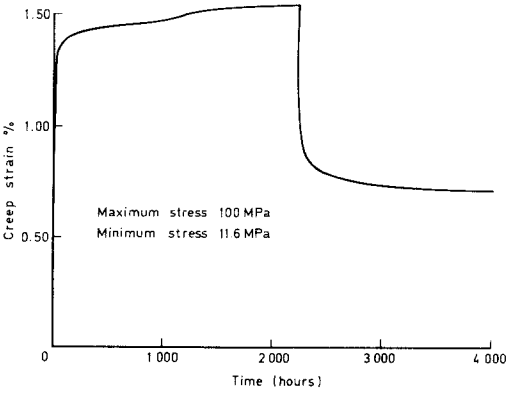

Figure 3 Creep and recovery strains for ± 45° CFRP tested at 21° C.

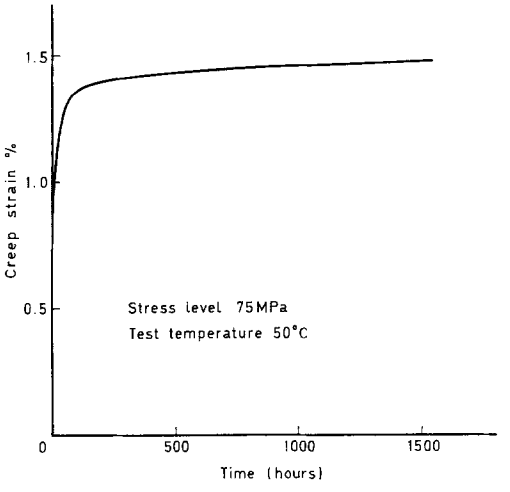

Figure 4 Creep strain for ± 45° CFRP tested at 50° C.

occur after continuous and repeated loading. The greater the number of repeated loading cycles the greater the permanent deformation. This behaviour is not unique to ± 45° CFRP having been reported for intermittent compressive creep tests on unreinforced polycarbonate [7] and in bituminous materials [8].

A rise of 30° C in the ambient temperature produces a significant increase in the overall creep strain but causes no alteration in the general shape of the creep curve. A plateau of nearly constant creep rate is still established, though at a larger strain than in a room temperature test. Fig. 4 gives a typical example of creep at 50° C and 75 MPa.

No evidence of any creep-rupture or tertiary creep behaviour has been detected as yet.

4. Fatigue tests

4.1. The fatigue specimen and testing technique

A simple rectangular specimen was used throughout since this is quite satisfactory for ± 45° orientations of CFRP [6]. The dimensions were 250 × 40 × 2 mm and thin aluminium end tabs were bonded to each end to prevent premature failure in the test machine wedge grips. The unsupported length was 170 mm.

All monotonic and fatigue tests were made in a Mayes servohydraulic testing machine type ESH 100D. A particular advantage of this machine is its memory modules which allow continuous monitoring of peak load and actuator position. Thus, changes in stiffness during a fatigue test can be followed continuously by recording the actuator position and displacement. A check at slow speeds revealed a linear relationship between actuator displacement and strain, up to strains where cracking began, as measured by a strain gauge mounted on the centre of a specimen.

4.2. Fatigue test results

All fatigue loadings were zero-tension, $P \pm P$, and the data is given as an S–log N curve in Fig. 5. Monotonic strength values are included at the half-cycle point. Initially all tests were made at 10 Hz which led to considerable heating at high stress levels (Fig. 6) so a few tests were repeated at 1 Hz. These showed reduced heating (Fig. 7) but little change in lifetime. Both heating curves have similar shapes showing an early rapid rise, a period of slow increase and finally another quite rapid rise in temperature as the specimen begins to fail.

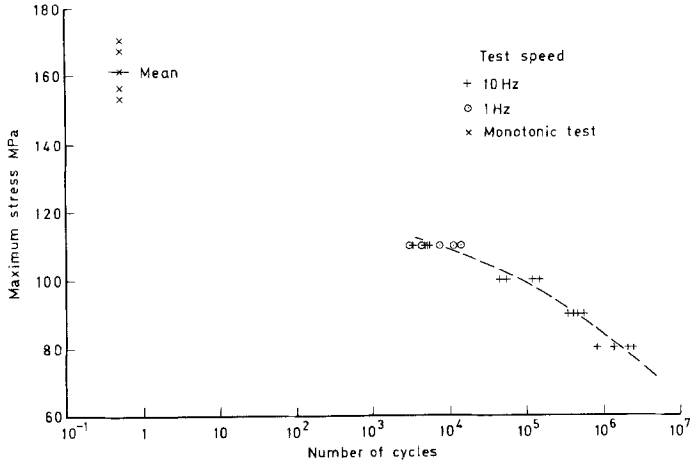

Figure 5 S–log N curve of zero-tension fatigue tests on ± 45° CFRP.

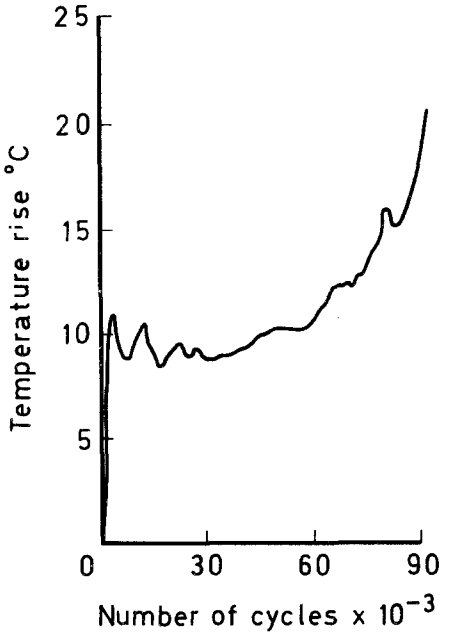

Figure 6 The temperature rise at 10 Hz during the fatigue testing of ± 45° CFRP over a stress range 8–94 MPa.

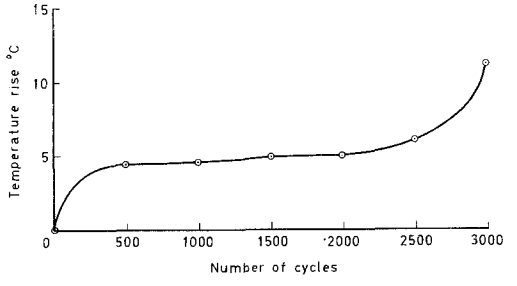

Figure 7 The temperature rise at 1 Hz during the fatigue testing of ± 45° CFRP over a stress range 0–110 MPa.

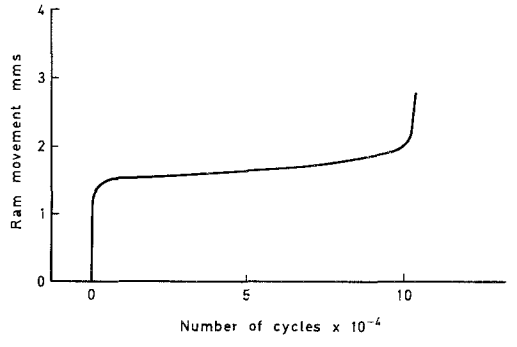

Figure 8 A trace showing the position of the fatigue machine ram at maximum load during fatigue testing of ± 45° CFRP over a stress range 0–90 MPa.

4.3. Creep during fatigue

Fig. 8 is a typical trace of the actuator position at maximum stress during a test over the range 0–90 MPa. An idealized form of this curve is represented with annotation in Fig. 9. The first part from 0–B is one of rapid change in specimen length followed by a longer period of slow change from B–D. Up to this point the curve is similar to the ordinary creep curve but here the analogy ends. In fatigue tests the increased displacement beginning at D marks the onset of cracking which ultimately leads to failure. No similar tertiary creep has been observed under prolonged static loadings.

Records of actuator position at zero load also reveal an increase in length showing that the deformation is not simply a softening of the dynamic response but true creep. Small changes in dynamic stiffness do occur but these are insignificant compared with the fatigue-induced creep; nevertheless, they follow a similar pattern showing increases just before the specimen fails. There is an interesting correlation between temperature rise and displacement with rapid changes in displacement being accompanied by similar changes in temperature.

An interrupted fatigue test with recovery periods was made to investigate the nature of fatigue-induced creep. The data for a specimen fatigued over a stress range of 0–100 MPa is given in Table II. On first loading the instantaneous strain was 1.11%. Clearly, the displacements consist of a recoverable component and a permanent deformation like the constant load creep tests.

Cyclic fatigue loadings were also applied to plain rectangular specimens of Shell 828/MNA/BDMA, an anhydride cured bis-phenol A epoxy-resin system but not identical with the DX210 system used in the laminates. Fatigue-induced creep strains were observed, similar to the com-

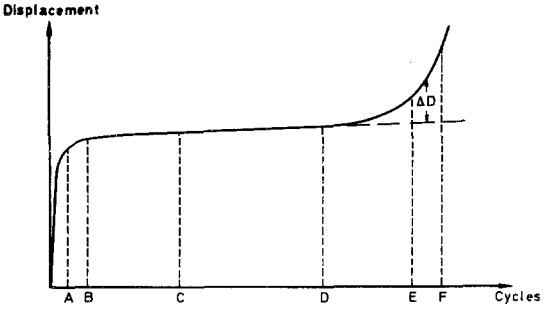

Figure 9 Displacement with cycles for ± 45° CFRP (letters indicate interrupted test positions).

TABLE II Creep and recovery during fatigue testing of ± 45° CFRP

Number of cycles sustained N	Total strain at N cycles (%)	Creep strain at N cycles (%)	Instantaneously recovered strain (%)	Recovery time (T_R) (h)	Creep strain recovered after T_R (%)	Permanent deformation after T_R (%)
1000	1.477	0.367	1.267	3.75	0.044	0.166
20 800	1.999	0.889	1.311	16.00	0.133	0.555
75 000	2.454	1.344	1.440	22.00	0.122	0.892

posite, but without any tertiary creep before failure. Instead failure was rapid and unexpected and the displacement plot was typical of Fig. 9 up to point D. Interrupted fatigue tests could not be made at the same strains as used above in the composite because the resin was too brittle and 0.5% strain had to be used instead for the specimen to survive a reasonable number of cycles. At this level all the fatigue-induced creep strain quickly recovered once the load was removed and no permanent deformation occurred. Further work is required to determine whether the permanent deformation in the composite results from high local resin stresses which cannot be simulated easily in bulk resin or whether they are indeed a characteristic of composites and not pure resin.

Finally no change in displacement was observed with a short aluminium alloy specimen showing that the creep was a real effect and not simply due to fretting in the grips.

4.4. Fatigue cracking in ± 45° CFRP

Some specimens were fatigued for a proportion of their lifetimes, corresponding approximately to points A–F on Fig. 9. After cycling they were sectioned, polished and photographed under a microscope. Those taken to A, B and C showed little or no sign of cracking. The few cracks which were present were probably formed on cooling during manufacture of the laminate, as frequently happen [3], or early in the fatigue life but they were very small and did not appear to be propagating significantly. At point D a number of intralaminar cracks appeared, perpendicular to the plane of the plies, (Fig. 10) becoming more numerous with further cycling to point E. The section made on the specimen taken to point F showed extensive interlaminar cracks in addition to the many intralaminar failures, Fig. 11.

It is clear that the first cracks to appear and propagate are intralaminar. These increase in size until a boundary between two plies is reached. If the plies have the same orientation the crack is very likely to propagate from one into the next. However, if the laminae are orthogonal the crack usually turns at the interface to become interlaminar. Sometimes it may continue into the second ply. This second case occurs when there is very little resin at the interface and no obvious boundary. At a resin-rich interface interlaminar cracks are much more likely.

Once interlaminar cracks have formed the plies

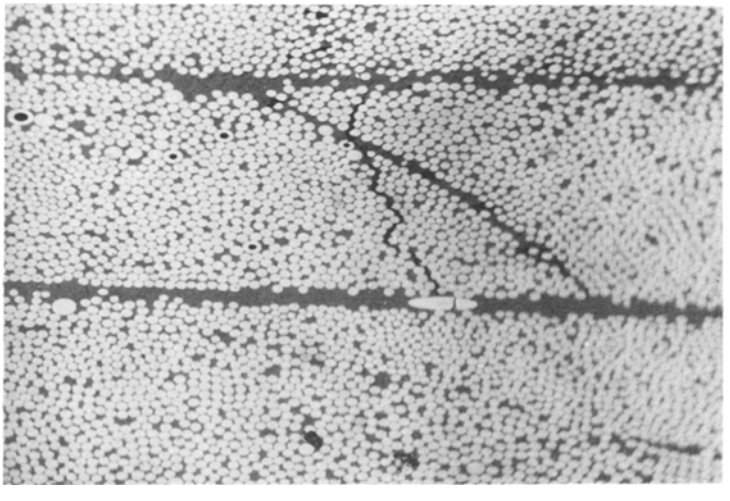

Figure 10 Intralaminar cracking becoming significant at point D of Fig. 9.

Figure 11 Extensive intra- and inter-laminar cracking corresponding to point F of Fig. 9.

move relative to one another in a scissoring action allowing correspondingly larger displacements. The combination of increased cracking coupled with scissoring explains the large displacements observed just before separation at failure.

5. A quantitative assessment of fatigue damage in ±45° CFRP

When metals are subjected to cyclic fatigue stresses the first signs of damage are a number of micro-cracks. Then, usually, one of these develops into a significant crack which propagates across the material resulting in failure. The problem of fatigue life prediction is, therefore, one of estimating the number of cycles to initiate a crack and then explaining its subsequent propagation and growth. Assessment of fatigue crack growth by fracture mechanics techniques is now quite widespread.

Reinforced plastics, on the other hand, usually contain many fatigue cracks. This is particularly true of oriented laminar constructions where, even if a stress-raiser such as a hole is introduced, many cracks form instead of a single dominant failure. Thus the basic concepts of fracture mechanics, which describe the growth of a single crack, must be modified or even discarded when considering composite materials. Two major types of cracking can be identified. These are (a) cracks where fibres are broken and (b) cracks where only the matrix or resin–fibre interface is damaged. Type (b) cracks dominate the early stages of damage in ±45° materials and an empirical approach can be used to assess the growth of damage in the material. This is discussed below.

The plot of Fig. 8, showing maximum displacement as a function of number of cycles, is useful for identifying crack initiation but not for analysis of crack growth. Instead a plot of log displacement attributable to cracking alone (ΔD) with log remaining lifetime (N_R) is more suitable because it emphasizes behaviour in the last few cycles rather than the first few decades [9]. It also has the advantage that, after the specimen has failed, the value of N_R and ΔD can be accurately measured by working back from the failure point on the recorded time versus displacement trace thus eliminating the difficulty of assessing accurately the position of point D, Fig. 9. The cracking displacement ΔD remains when the creep component, assumed linear, is subtracted from the total displacement (Fig. 9).

Plots of log ΔD against log N_R are given in Figs. 12 and 13 for specimens tested in the range 0–90 MPa and 0–80 MPa respectively. These stress levels were chosen because heating effects are small at 10 Hz so the data are almost isothermal. Fig. 12 contains results from four specimens. Data from only one specimen are given in Fig. 13. Unfortunately jamming of the chart recorder made the other 80 MPa data unreliable and no identical material was available for further testing. In both cases a straight line relationship is obtained.

It is reasonable to assume that the increase in displacement ΔD caused by cracking is related to the following quantities; (i) the overall length L of the test-piece, (ii) the total number of cracks, C, already present in the test-piece (it is assumed that C is never zero in a composite, that is that

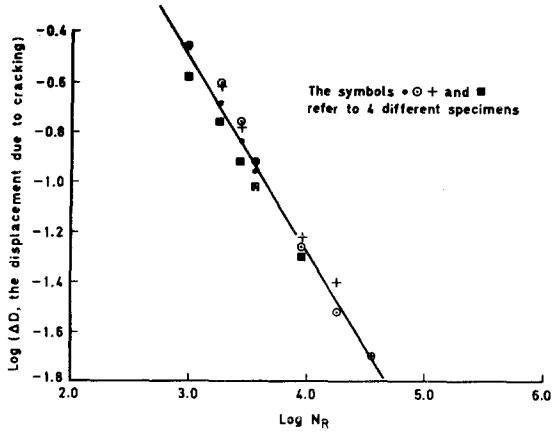

Figure 12 A plot of log (ΔD, the displacement due to cracking) versus log N_R for four specimens tested over a stress range 0 to 90 MPa.

cracks already exist when the point D of Fig. 9 is reached), (iii) a crack opening compliance β, and (iv) the maximum stress σ_{max}. This latter determines how far the cracks open and combined with the stress range $\Delta\sigma = \sigma_{max} - \sigma_{min}$, determines the rate of growth of cracking.

An expression of the following form may be postulated

$$\Delta D = L\beta f(\sigma_{max}\Delta\sigma)C^{\omega} \qquad (1)$$

where ω is a constant and $f(\sigma_{max}\Delta\sigma)$ is some function of the stress range and the maximum fatigue stress.

Now, Figs. 12 and 13 show that ΔD and N_R are related by an equation of the form

$$\log \Delta D = m_\sigma \log N_R + \log A_\sigma \qquad (2a)$$

or

$$\Delta D = A_\sigma N_R^{m_\sigma} \qquad (2b)$$

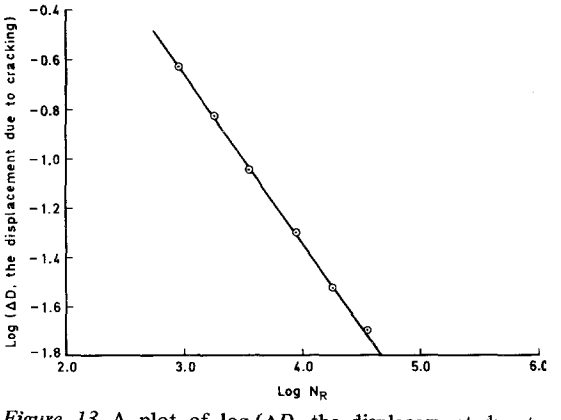

Figure 13 A plot of log (ΔD, the displacement due to cracking) versus log N_R for one specimen tested over a stress range 0 to 80 MPa.

where m_σ is the slope of the log–log plot for the particular value of applied stress σ, and A_σ is a constant at the same value of σ. In a general equation it must be assumed that both m_σ and A_σ are functions of the applied stress.

Equation 2 applies only when cracking has begun, i.e. after point D in Fig. 9. To simplify the analysis it will be assumed that ΔD is directly proportional to the number of cracks, i.e. $\omega = 1$. In this case substituting Equation 2b into Equation 1 gives

$$L\beta f(\sigma_{max}\Delta_\sigma)C = A_\sigma N_R^{m_\sigma}$$

or

$$C = \gamma N_R^{m_\sigma}$$

where

$$\gamma = \frac{A_\sigma}{L\beta f(\sigma_{max}\Delta_\sigma)}.$$

Thus, the increase in cracking per cycle of remaining life $\partial C/\partial N_R$ is given by

$$\frac{\partial C}{\partial N_R} = m_\sigma \gamma N_R^{(m_\sigma - 1)}$$

which on substituting for N_R gives

$$\frac{\partial C}{\partial N_R} = m_\sigma \gamma^{1/m_\sigma} C^{(m_\sigma - 1)/m_\sigma}$$

$$= m_\sigma \left(\frac{A_\sigma}{L\beta}\right)^{1/m_\sigma} [f(\sigma_{max}\Delta\sigma)]^{-1/m_\sigma} C^{(m_\sigma - 1)/m_\sigma} \qquad (3)$$

Values of m_σ and A_σ, determined by a least squares regression analysis, are given in Table III below for two stress ranges, 0–80 MPa and 0–90 MPa.

The form of Equation 3 could be verified by direct observation of cracking during a test. Unfortunately this is a difficult task. The observation cannot be made whilst the test is in progress since many cracks, not just one, must be observed. Also only cracks visible at the edge of the test-piece will be detected and estimating the total crack volume is not easy. Non-destructive testing methods, such as ultrasonics, may be suitable for this estimation.

TABLE III Experimentally determined values of m_σ and A_σ

Maxium applied stress (MPa)	m_σ	A_σ
80	–0.674	23
90	–0.776	66

6. Discussion

Equation 3 shows some similarity to the fracture mechanics equation which is often used to describe the crack growth rate of a single crack namely

$$\frac{\partial a}{\partial N} = B(\Delta K)^n \qquad (4)$$

where a is half the crack length, B and n are constants and ΔK is the stess intensity range given by

$$\Delta K = \Delta\sigma\sqrt{(\alpha\pi a)}$$

where $\Delta\sigma$ is the stress range and α is a geometrical factor, often set equal to unity. This equation can also be written in the form

$$\frac{\partial a}{\partial N} = \text{const}\,(\Delta\sigma)^n a^{n/2}$$

or more generally

$$\frac{\partial a}{\partial N} = \text{const}\, f(\Delta\sigma)g(a) \qquad (5)$$

if $f(\Delta\sigma)$ is some function of stress range and $g(a)$ is a function of crack length or, expressed in another way, the total amount of cracking.

In the derivation leading to Equation 3 no assumptions were made on the validity of a stress intensity factor K for composite materials. Nevertheless Equation 3 is generally similar to Equation 5 because the growth rate of the total number of cracks is dependent both on the stress and the number of cracks already present. The cracking is more complex in composites than in homogeneous isotropic materials, witness the simpler stress intensity factor relationship of Equation 4.
cept is the existence of a clearly defined function K, which has physical significance. Where there are a limited number of cracks interacting with each other in isotropic materials the concept is valid. But it is not necessarily useful in composites where several failure mechanisms operate simultaneously. In this latter case a general relation is more suitable and the problem then becomes one of identifying the appropriate functions. The equation which describes the cracking behaviour of ±45° CFRP is

$$\frac{\partial C}{\partial N_R} = F(\sigma_{max}, \Delta\sigma)G(C, \sigma_{max})$$

where $F(\sigma_{max}, \Delta\sigma)$ is a function of the maximum stress and the stress range and

$$G(C, \sigma_{max}) = C^{(m_\sigma - 1)/m_\sigma}$$

This relation is more complex than Equation 5 involving the maximum stress in each function F and G as well as stress range and amount of cracking.

From a practical point of view the paper has shown two things; that creep occurs during static and repeated loading of ±45° orientations and that cracking becomes significant relatively late in the fatigue endurance. As expected, cracking is accompanied by a general decrease in specimen stiffness but only when interlaminar cracks develop is failure imminent. Non-destructive testing methods which detect this particular failure may therefore be useful in determining when a component, subjected to more realistic loadings than constant amplitude, is no longer serviceable.

7. Conclusions

Creep effects in ±45° CFRP are significant at room temperature when the material is subjected to both static and fluctuating tensile stresses. Creep strain is composed of a permanent and a recoverable component in both cases.

Cracking occurs in cyclic fatigue. Its growth rate at constant temperature is dependent on both stress and the amount of cracking already present. The simple stress intensity factor approach to crack growth is not appropriate for composite materials, but a more general modified equation can possibly be used in the form

$$\frac{\partial C}{\partial N_R} = F(\sigma_{max}, \Delta\sigma)G(C, \sigma_{max}).$$

Acknowledgement

The creep and intermittent loadings were made by Mr. R. L. Butt and L. W. Larke of Materials Department, Royal Aircraft Establishment. This paper is printed by the kind permission of the controller HMSO.

References

1. J. B. STURGEON, 28th Annual Technical Conference, Reinforced Plastics/Composite Division, The Soc. of Plastics Industry, Washington DC, Paper 12-B (1973).
2. M. J. OWEN and S. MORRIS, 25th Annual Technical Conference, Reinforced Plastics/Composite Division, The Soc. of Plastics Industry, Washington DC, Paper 8-E (1970).
3. *Idem,* International Conference on Carbon Fibres, their Composites and Application, London, The Plastics Institute, Paper 51 (1971).
4. L. G. BEVAN and J. B. STURGEON, 2nd International Conference on Carbon Fibres, their place in

Modern Technology, London, The Plastics Institute, Paper 32 (1974).
5. H. T. SUMSION and D. P. WILLIAMS, Fatigue of Composite Materials, ASTM STP 569, Philadelphia, Pa, The American Society for Testing and Materials (1975).
6. J. B. STURGEON, Proceedings of the International Conference on fatigue, City University, London, Paper 11 (1976).
7. M. J. MINDEL and N. BROWN, *J. Mater. Sci.* 8 (1973) 863.
8. S. F. BROWN, "Creep of Engineering Materials" (Institute of Mechanical Engineers) to be published.
9. R. R. FUJCZAK, Watervliet Arsenal Report TR 74006 (1974).

Received 30 May 1977 and accepted 13 September 1977.